Intehaa A. Mohammed [1]
Anaam W. Watan [1]
Jaafar S. Mohammed [2]
Kareem A. Jasim [1]
Firas K. Nsaif [1]
Auday H. Shaban [3]

[1] *Department of Physics, College of Education for Pure Sciences / Ibn Al-Haitham, University of Baghdad, Baghdad, IRAQ*
[2] *Department of Physics, College of Science, University of Diyala, Diyala, IRAQ*
[3] *Department of Remote Sensing & GIS, College of Science, University of Baghdad, Baghdad, IRAQ*

Effect of Partial Substitution of Selenium with Copper on Conduction Mechanism in $Ge_{20}Se_{80-x}Cu_x$ Alloy

Chalcogenide glass alloys are actively pursued worldwide because they are applicable in various technologies owing to adequate amorphous semiconducting features. Chalcogenide system $Ge_{20}Se_{80-x}Cu_x$ with x = 0, 5, 10, and 15 were prepared by melt quenching method, and the effect of partial replacement of selenium with copper on the electrical and optical properties was studied. The results showed that there are three types of electrical conduction: the first occurs between the local states near the Fermi level at low temperatures, the second occurs at intermediate temperatures between the local state of the tails of the energy gap, and the third occurs between the extended state of the valence and conduction bands at high temperatures.

***Keywords*:** Chalcogenides; Glass alloys; Conduction mechanisms; Fermi states
Received: 26 December 2023; **Revised:** 22 January; **Accepted:** 29 January 2024

1. Introduction

Chalcogenide glasses consist of basic chalcogens such as sulfur (S), selenium (Se) and tellurium (Te) belonging to subgroup VI-A of the periodic table, mixed with electronegative elements or with organic radicals. The word chalcogenide is derived from a combination of the following Greek words: “copper”, “born”, and “type” [1]. Among inorganic glasses, chalcogenide glasses form an important class due to their technological applications in a wide range of fields such as biosensors [2], night vision cameras [3], switches, and microelectronics of infrared devices [4]. Chalcogenide glasses also have strong technical interest since some amorphous alloys of selenium exhibit several anomalous features such as negative viewing efficiency [5], large shift in the Fermi level and large photoelectric effect [6] Efforts have also been made by many scientists and researchers from time to time to study the chemical composition [7]. Studies on the temperature dependence of the conductivity of chalcogenide glasses have provided ways to effectively control the conductivity of amorphous semiconductors [8]. The electrical transport properties of a material are of great importance in determining whether a material is compatible with our practical needs or not [9]. Therefore, we find it useful to study the electrical conductivity dependence on the temperature of the $Ge_{20}Se_{80-x}Cu_x$ chalcogenide glass system (x = 0, 5, 10, and 15) and the effect of increasing the partial substitution ratio (x) according to the density of both local and extended states and its effect on the physical properties and their improvement for further scientific applications.

2. Experimental Part

Using molten cooling technology, a $Ge_{20}Se_{80-x}Cu_x$ glass alloy with x = 0, 5, 10, and 15 was fabricated. The components of the alloy, consisting of pure elements (99.99% of germanium (Ge), selenium (Se), and copper (Cu), are weighed and mixed using an electric grinder, then placed in quartz ampoules (10cm long and about 1.5cm inner diameter) and closed after being emptied to 10^{-4} bar. The sealed ampoules are placed in a furnace heated to 950°C at a rate of 5°C per minute. To ensure the homogeneity of the ingredients, the ampoules are shaken continuously for an hour at the highest temperature. Then the ampoules are taken out of the furnace and placed in freezing water to cool. Then each urine is broken individually. These alloys are ground into fine powders and then pressed using a hydraulic press. The powder is compressed under a force of about 6 tons/cm^2 to produce large disc-shaped samples, 1.5cm in diameter and 0.2cm thick. The temperature is measured by mounting a thermocouple near the sample in a specially designed metal sample holder. Current is measured with a digital meter by applying a constant current voltage across the sample with a change in the approved temperature. To determine each sample's conductivity for each value of x. Electric current is passed along the sample area's plane to naturally flow through the sample area's cross-section rather as opposed to running parallel to

its surface. For each change in the sample temperature in the oven, record the current (in amperes) and voltage (in volts) all at the same time using the thermal cable. With each of these steps, we calculate the electrical conductivity versus temperature. Amorphous semiconductor materials have states localized within the energy gap because the edges of the valence and conduction bands extend into the energy gap [10]. These cases can be very or sparsely dense, depending on the type of material, composition, preparation technique, and variables present during the process. As a result, scientists have introduced several models - the most famous of which are the Mott-Davis and Cohen-Farish-Ovshamsky models - to explain the mechanisms of conduction in these substances [11]. According to Cohen-Farish-Ovshamsky [12], the edges of the electricity and charge-tails overlap each other across the energy gap. As a result, the density of energy states expands to the center of the energy gap, where the conduction and valence edges eventually touch to close the gap [13]. Since the levels of the conduction band transitions are frequently devoid of electrons, the tails of the conduction band are filled with empty states of electrons as a result of electron redistribution caused by interference between the edges of these bands [14]. The valence band states, on the other hand, are neutral and constantly contain electrons at their edges. There are electrons in the tails that are close to the valence band states [15]. The tails' interference causes positively charged states to emerge while the interference region takes on a negative charge. The Fermi level will remain in the middle of the energy gap thanks to this distribution. Rotation to one side will occur if charges are present inside the gap. Figure (1a) shows the distribution that this model represents. Two major issues with this method are the lack of a single cycle and the chalcogenide glasses' extremely high degree of transparency. This concept does not apply to chalcogenide glasses due to the narrow tails of the valence and conduction bands in these materials. The Moot and Davis model [11] predicts that the energy gap in the conduction and valence bands is small, narrow, and lies in a short range close to the band edges; They reach a maximum of a few tenths of MeV. According to this model, the narrow region at the edges of the valence and conduction bands is all that the conduction and valence band edge tails extend to. Only a few tenths of an electron volt separates these two energy states.

In Fig. (1b), it can be observed that level bands caused by defects like hanging bonds and holes (particularly in chalcogenide glasses) appear close to the energy gap's center when E_A and E_B are used to distinguish between the local and extended states. The Moot and Davis model is the best fit for explaining the existence of energy levels in chalcogenide glasses, which are symbolized by the local extended level and the Fermi level because the kinetic energy of the electrons between local levels decreases as they move from extended to local states. Because of this, the electrical conductivity of chalcogenide glasses can be determined over three temperature ranges: low, medium, and high [15]. Therefore it shows dc conductivity depending on temperature. These three regions do not need to be present in every chalcogenide compound, as this depends on the amount of randomness in the crystal structure. The Moot and Davis model can be expressed by the following relationship [11]:

$$\sigma = \sigma_{01} e^{-\frac{E_1}{k_B T}} + \sigma_{02} e^{-\frac{E_2}{k_B T}} + \sigma_{03} e^{-\frac{E_3}{k_B T}} \qquad (1)$$

where T is the absolute temperature, E_1, E_2, and E_3 are the activation energies of each term, the preceding pre-exponential factor parameters are σ_{01}, σ_{02}, and σ_{03}, and k_B is the Boltzmann constant

Equation (1) includes distinct conduction mechanisms for each temperature zone; the high temperature (HT) region is represented by the first term, while the intermediate (IMT) and low temperature (LT) zones are represented by the second and third terms, respectively. By computing the logarithm of both sides of Eq. (1) and displaying ($\ln\sigma_{dc}$) versus (1000/T) on a graph, we can obtain three distinct straight lines with various slopes that correspond to the three components of Eq. (1).

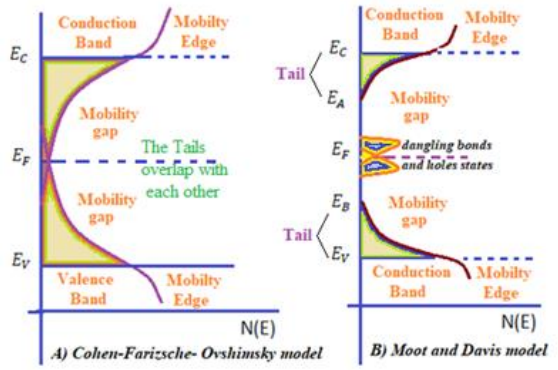

Fig. (1) Cohen-Farizsche-Ovshimsky model (A) and Moot and Davis model (B)

3. Results and Discussion

The logarithm of dc electrical conductivity ($\ln\sigma_{dc}$) results were plotted as a function of the reciprocal temperature of the $Ge_{20}Se_{80-x}Cu_x$ system (where x = 0, 5, 10, and 15). Figure (2) demonstrates the reliance of $\ln\sigma_{dc}$ on the exchange temperature in the range 300 to 475°C. All samples show common patterns in which three regions of conductivity are observed. It is noted from this figure that σ decreases with decreasing temperature which indicates the increase in the density of localized states. The activation energy and previous exponential factors were estimated for the three regions and were included in the table (1).

Figure (2) shows the effect of the Cu content on the value of the σ and it is clear that σ has a direct relationship with the Cu content. This indicates that the addition of the Cu leads to an increase in the density of the local states. To validate the

compensation law, the previous exponential factor σ_0 versus the activation energy (E_a).

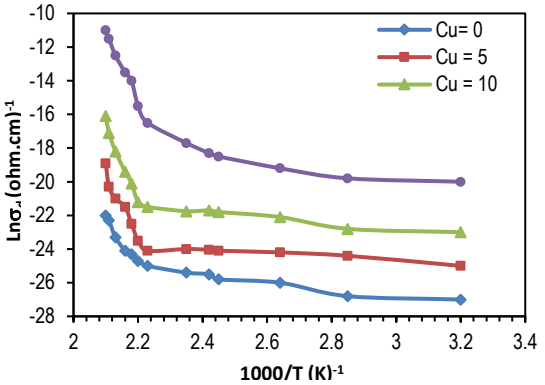

Fig. (2) Relationship between the logarithm of the dc electric conductivity ($\ln\sigma_{dc}$) and the reciprocal of the absolute temperature (1000/T) for the $Ge_{20}Se_{80-x}Cu_x$ chalcogenide glass system at various Cu concentrations

This figure demonstrates that there are three zones for each sample of the $Ge_{20}Se_{80-x}Cu_x$ formulations depending on the variation in the logarithmic value of the dark conductivity ($\ln\sigma_d$) with (1000/T) for each value of x. This in turn means that three different conduction mechanisms dominate over specific temperature intervals in the extended and localized region and at the Fermi level. The $\ln\sigma_d$ versus 1000/T curves are straight lines in the Three measurement temperature ranges (300-360, 360-400 and 400-475K). This indicates that the conduction in these samples is through three conduction processes, one at high temperatures (400-475K) and the other at low temperatures (300-360 and 360-400K) as shown in Fig. (2). And that there are three activation energies for each x ratio in the temperature range examined. Thus, σ_d can be expressed by the usual Eq. (1).

In addition to extrapolating each line intercepting the y-axis with a value equal to ($\ln\sigma_d$) (with x = 0, 5, 10 and 15) pre-exponential factors can be calculated. The data were obtained for each of the pre-exponential factor parameters (σ_{01}, σ_{02}, σ_{03}) and activation energies (E_1, E_2, and E_3) and the tail width ΔE were recorded in the table (1). We noted from pre-exponential factors (σ_{01}, σ_{02}) that the activation energies in the extended and localized regions increase with increasing concentration of the copper in the samples. While σ_{03} and ΔE_3 oscillate between up and down in the local state inside the energy gap. In addition to that fact, the width of the tails changed with increasing the Cu concentration.

It can be seen from Fig. (2) that the first region (HT) is confined between 400 and 475K and is determined by the first part in Eq. (1) the high-temperature region. In this region, the carrier density is the same as the intrinsic carrier density [16]. Here, lattice vibrations and sample temperature influence the transformation. Temperature increases the number of charge carriers (electrons and holes), which increases conductivity. On the other hand, phonons generated by the vibration of the lattice lead to an electrical interaction. Electrons become trapped as a result of this process, requiring more energy to activate them [17]. This explains the high activation energy values in the first region [18]. The second zone begins with a temperature from 360 to 400K (intermediate temperature zone). This region is described by Eq. (1) second term and defined as an intrinsic semiconductor. Within this region, the carrier's density is equal to eigenvectors [19]. The variability of the dc conductivity in this region is due to the change in the mobility, the mean free path of the charge carriers, and their concentration. This can also be explained by the low degree of crystallinity and the small size of the crystals. The presence of defects such as skeletal disorders and disorders resulting from the drooping ligaments, the randomness in the structure, and the surface defects also played a key role in reducing the conductivity as reported in the literature [20].

The third region is known as the low-temperature region (LT), which represents the third term of Eq. (1), starting from room temperature to 360 K, where this temperature provides the impurities with energy until they reach depletion temperatures. It is also known as the external conductivity of the semiconductor due to the ionization of the impurity atoms. In the low-temperature range, data have indicated that the conduction attributed to interstate carrier-assisted hopping approaches the Fermi level [21]. Activation energies, ΔE_1, ΔE_2, and ΔE_3, were calculated from the slope of the straight lines in Fig. (2) for each conduction region. The activation energies and exponential pre-factors of three regions for each sample were estimated from the triangular $Ge_{20}Se_{80-x}Cu_x$ array and then recorded in the table (1).

The values of E_1 rise linearly with increasing concentrations of Cu as shown in Fig. (3). This effect is likely due to the reduction of average the binding energy by Cu addition, while the E_2 and E_3 values decrease linearly with increasing concentrations of Cu. This effect is likely due to the reduction of average binding energy by the addition of Cu. The presence of three conduction regions (three conduction mechanisms) in these samples suggests the presence of a large amount of electrically active defects within the bulk material, but a clear understanding of the fundamental mechanisms underlying their electrical conductivity is currently still missing [21]. In a first step towards elucidating their conduction mechanism, this work focuses on the measurements of electrical conductivity of the glass $Ge_{20}Se_{80-x}Cu_x$ compounds to determine the effect of the copper addition on contribution to the defect formation and its effect on density of the localized and extended states in the three Regions; low, medium and high temperature. So we will calculate the density of each case separately.

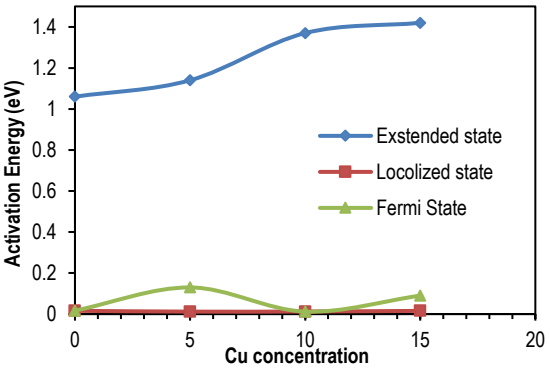

Fig. (3) The activation energy determined by the Cu concentration in $Ge_{20}Se_{80-x}Cu_x$ chalcogenide glass system (x = 0, 5, 10 and 15)

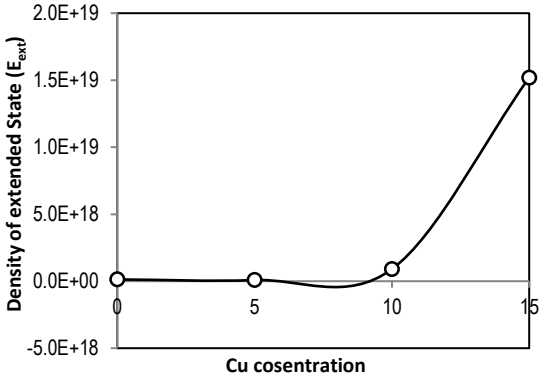

Fig. (4) Density of the extended state (E_{ext}) as a function of the Cu concentration in $Ge_{20}Se_{80-x}Cu_x$ chalcogenide glass system (x = 0, 5, 10 and 15)

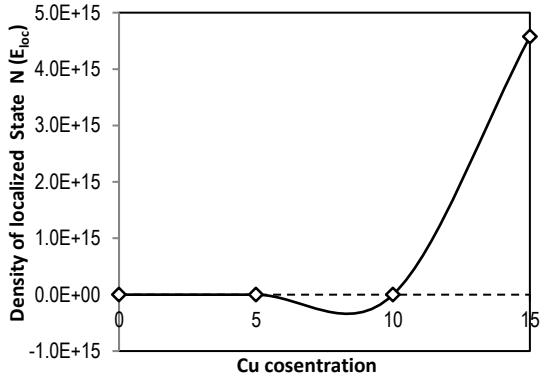

Fig. (5) Density of the localized state $N(E_{loc})$ as a function of Cu concentration in $Ge_{20}Se_{80-x}Cu_x$ chalcogenide glass system (x = 0, 5, 10 and 15)

The high-temperature region can be provided by the exponential temperature dependence of the first part of Eq. (1), where this correspondence appears on the first segment of the curve in Fig. (2). This exponential dependence is consistent with an activated process due to the conduction of the expanded state after the electronic excitation across the band gap (E_c–E_v). Depending on the pre-exponential factor σ_{0ext}, this can be represented by the Eq. (2) [17]. The density of states in the extended region $N(E_{ext})$ and for all samples when increasing concentration of the copper can be calculated as shown in Fig. (4) and the dates are noted in table (2). It is noted from this table that an increase in the concentration of copper in the samples led to an increase in energy levels in the extended cases, this is evident in increase in tail width as shown in table (2).

$$\sigma_{0ext.} = \frac{1}{6} e^2 v_e a^2 N(E_{ext}) \qquad (2)$$

Electron frequency is $v_e = \frac{\hbar}{a^2 M}$, interatomic distance $a = 0.026 \frac{e^2}{\hbar \sigma o}$, electron charge ($e$) and density of the extended states $N(E_{ext})$

The pre-exponential factor σ_{02}that precedes the exponent in the mean temperature region can also be obtained from the mean curve in Fig. (2) and table (1). This exponential dependence in the mean temperature region corresponds to the transfer by the excited carriers to the local states followed by hopping. Using the results obtained for pre-exponential factor σ_{0loc} from the table (1) and applying Eq. (3) which is derived in references [17], the density of the energy states in the local region $N(E_{loc})$ was calculated and recorded in table (2). It is noticed that the values of $N(E_{loc})$ increase with the increase in the copper concentration as shown in Fig. (5) and this explains that the randomness increases with the increase in the copper concentration.

$$\sigma_{02} = \frac{e^2 V_{ph} R^2 N(E_{loc})}{6} \qquad (3)$$

where R is the distance between two localized states and V_{ph} is a phonon frequency

The $N(E_{loc})$ values for positional state conductance are four to six orders of magnitude lower which is also in line with expectations for this type of conductivity. The decrease in the activation energy is also consistent with the expectation for such glasses [18].

Conduction at very low temperatures is called variable band hopping (VRH) and involves phonon-assisted tunneling of charge carriers in localized defect states. This type of temperature-dependent conductivity follows according to the third part of Eq. (1).

The histogram of low-temperature conductivity for the four most prominent samples is shown in Fig. (2) as a function of the reciprocal of absolute temperature (1000/T). Each curve shows a linear dependence on the inverse of its temperature confirming the VRH type of conduction in the temperature range [19]. From the parameters σ_{03} and conductivity VRH in table (1), the local densities of states of the Fermi level $N(E_F)$ were calculated using Eq. (4) [20,21]. The results were recorded in table (2).

$$\sigma_{03} = \frac{e^2 V_{ph} R^2 N(E_F)}{6} \qquad (4)$$

Throughout these results, it is noted that there is a slight increase in density of the localized states at the Fermi level. It can be said that increasing the concentration of the copper has a very small effect on $N(E_F)$ as shown in Fig. (6), but significantly on $N(E_{ext})$

and this explains that the randomness in the composition has decreased significantly [21]. It was found that the addition of Cu significantly reduces the activation energy of electrical conductivity and increases the overall conductivity. This is also the case for other chalcogenides mixed with copper such as Cu-As-Se glass and Cu-As-S glass [22,]. Unshared electron states are known as lone pair (LP) electrons. Kastner was the first to describe effects of the adding elements such as copper to V-VI alloys [23]. He noted that copper broadens the tail state in the valence band (LP band) because the LP electrons adjacent to the electronegative atoms will have higher energies than those near the electronegative atoms. In addition, the conduction band tail widens due to the increase in types of the bonds present in the alloy, and the broadening may not be the same with the LP band. The conduction band may also be affected by the establishment of the Ge-Se bonds that lower the conduction band edge.

At lower temperatures, the conductivity of the copper-rich glass is dominated by the varying range of mobility, and this type of conductivity results from the presence of the dangling bonds that generate electronic states within the gap [17]. The activation energy for an electron to jump to a neighboring empty state just above the Fermi level is small enough to observe conduction even at low temperatures [21]. This type of conductivity is usually only prominent in quickly quenched bottles such as films with a large amount of "frozen" defects [24]. However, the present results clearly show that the addition of Cu modifies the structure to allow more of these defects to exist even in annealed glass and prevents the formation of VAPs that convert dangling bonds normally into charge defects. Based on the conduction slope analysis, this type of defect contains unpaired electrons; hence, these glasses are expected to show a strong signal [25].

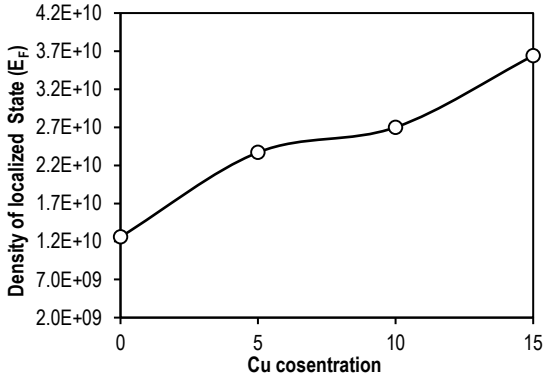

Fig. (6) Density of the localized state at Fermi level (E_F) as a function of Cu concentration in $Ge_{20}Se_{80-x}Cu_x$ chalcogenide glass system (x = 0, 5, 10 and 15)

Using the UV-visible spectrophotometer, the optical characteristics of $Ge_{20}Se_{80-x}Cu_x$ chalcogenide glass system (pure and partially replaced by copper) were studied with different replacement ratios (x = 0, 5, 10 and 15), and throughout the transmission and absorption spectra recorded for samples within the wavelength range 300-1100 nm.

Figure (7) depicts the change in the absorption spectrum as a function of wavelength since all samples have the highest absorbance at short wavelengths, then, as the wavelength increases, it lowers until it reaches its minimum in the visible region of the electromagnetic spectrum [26]. Because an incident photon cannot excite and move an electron from the valence band to the conduction band due to the photon's energy, these membranes can be employed as windows in solar cell applications. Because the drop is less than the semiconductor's energy gap value, the absorbance declines as wavelength increases [27]. Additionally, it is observed that the absorbance rises as the proportion of copper increases when compared to the pure sample. This is because the partial replacement of Se with copper increased the absorption by creating donor levels in the energy gap near the conduction and valence bands.

As shown in Fig. (8), the transmission spectra of all pure and partially replaced copper samples exhibits minimum transmittance at the fundamental absorption edge (short wavelengths), increases with an increase in wavelength, then exhibits an abrupt and significant increase to be constant at wavelengths longer than 360nm (visible and near-infrared regions). However, as the proportion of copper increases, the transmittance decreases as a result of the absorption by copper.

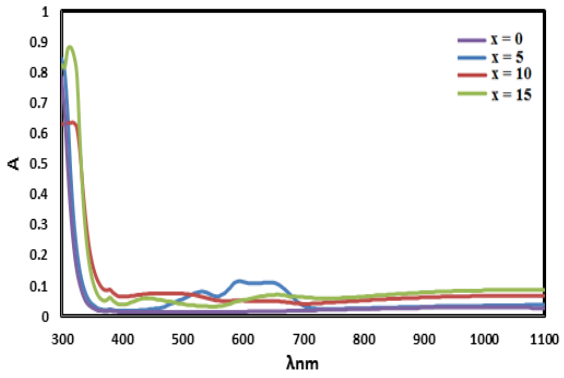

Fig. (7) Absorption spectra of $Ge_{20}Se_{80-x}Cu_x$ chalcogenide glass systems (x = 0, 5, 10 and 15)

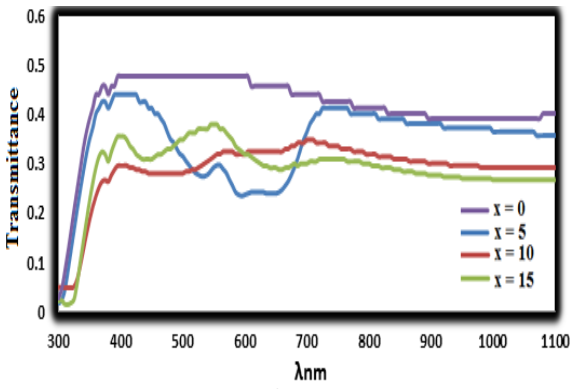

Fig. (8) Transmissin spectra of $Ge_{20}Se_{80-x}Cu_x$ chalcogenide glass systems (x = 0, 5, 10 and 15)

4. Conclusions

This work focused on the preparation and study of the electrical properties of the chalcogenide glass system $Ge_{20}Se_{80-x}Cu_x$ chalcogenide glass system (x = 0, 5, 10, and 15). It was found that there are three conduction mechanisms. Copper had the effect of increasing the activation energy for extended state conduction and reducing the activation shot in the gap localized states. Also, it was found that increasing the concentration of copper in the samples led to a clear change in all conduction coefficients, local and extended states, and at the Fermi level, and the optical properties of the glass system.

References

[1] A.A Wilhelm et al., "Biocompatibility of Te–As–Se glass fibers for cell-based bio-optic infrared sensors", *J. Mater. Res.*, 22(4) (2007) 1098-1104.

[2] Z. Yang, A.A Wilhelm and P. Lucas, "High-conductivity tellurium-based infrared transmitting glasses and their suitability for bio-optical detection", *J. Amer. Cer. Soc.*, 93(7) (2010) 1941-1944.

[3] P.S. Salmon, "Structure of liquids and glasses in the Ge–Se binary system", *J. Non-Cryst. Solids*, 353(32) (2007) 2959-2974.

[4] X.H. Zhang, Y. Guimond and Y. Bellec, "Production of complex chalcogenide glass optics by molding for thermal imaging", *J. Non-Cryst. Solids*, 326 (2003) 519-523.

[5] N. Mehta, "Applications of chalcogenide glasses in electronics and optoelectron-ics: A review", *J. Sci. Ind. Res.*, 65(10) (2006) 777.

[6] I. Watanabe and T. Sekiya, "Anomalous electrical conduction in amorphous In_2Se_3 films", *J. Non-Cryst. Solids*, 97-98 (1987) 667-670.

[7] T.T. Nang et al., "The photovoltaic effect observed on the construction of metal-amorphous In_xSe_{1-x} film System", *Japanese J. Appl. Phys.*, 16(2) (1977) 253-257.

[8] K.A. Jasim and R.N. Fadhil, "The effects of micro aluminum fillers in epoxy resin on the thermal conductivity", *IOP J. Phys.: Conf. Ser.*, 1003 (2018) 012082.

[9] K.A. Jassim, W.H. Jassim and S.H. Mahdi, "The effect of sunlight on medium density polyethylene water pipes", *Energy Procedia*, 119 (2017) 650-655.

[10] N.H. Khudhair and K.A. Jasim, "Study of the effectiveness of tin on the thermal conductivity coefficient and electrical resistance of $Se_{60}Te_{40-x}Sn_x$ chalcogenide glass", *Ibn Al-Haitham J. Pure Appl. Sci.*, 36(1) (2023) 149-157.

[11] N.F. Mott and E.A. Davis, **"Electronic Processes in Non-Crystalline Materials"**, Clarendon Press (Oxford, 1979) 591.

[12] M. Cohen, H. Fritzsche and S. Ovshlnsky, "Simple Band Model for Amorphous Semiconducting Alloys", *Phys. Rev. Lett.*, 22 (1969) 1065.

[13] A.N. Abdulateef et al., "Calculating the Mechanisms of Electrical Conductivity and Energy Density of States for $Se_{85}Te_{10}Sn_{5-x}In_x$ Glasses Materials", *J. Green Eng.*, 10(9) (2020) 5487-5503.

[14] R.K. Chillab et al., "Fabrication of $Ge_{30}Te_{70-x}Sb_x$ Glasses Alloys and Studying the Effect of Partial Substitution on D.C Electrical Energy Parameters", *Key Eng. Mater.*, 9 (2021) 163-171.

[15] H.A. Mahdi, K.A. Jasim and A.H. Shaban, "Manufacturing and improving the characteristics of the isolation of concrete composites by additive Styrofoam particulate", *Energy Procedia*, 157 (2019) 158-163.

[16] B.T. Kolomiets, B.L. Gelmont and K.O. Tsendin, "Impurity Conduction of Chalcogenide Vitreous Semiconductors", *phys. stat. sol.*, 91(1-3) (1985) 417-419.

[17] T.J. Alwan and K.A. Jasim, "The Influence of Annealing Temperature on Density of States, Electrical and Optical Properties of $Ge_{0.2}Te_{0.8}$Thin Film", *Mater. Sci. Technol.*, October (2010) 17-21.

[18] M. Kastner, "Bonding Bands, Lone-Pair Bands, Impurity States in Chalcogenide Semiconductors", *Phys. Rev. Lett.*, 28(6) (1972) 355-357.

[19] K.A. Jasim et al., "The effects of copper additives on the glass transition temperature and hardness for epoxy resin", *Prog. in Ind. Ecol.*, 13(2) (2019) 163-172.

[20] N.H. Khudhair and K.A. Jasim, "Study the Effect of Tin on the Energy Density of States of $Se_{60}Te_{40-X}Sn_x$ Chalcogenide Glass", *AIP Conf. Proc.*, 2769 (2023) 020062 (1-7).

[21] N.H. Khudhair and K.A. Jasim, "Preparation and Study the effective of Sb on the energy density of states of $Se_{60}Te_{40}$", *AIP Conf. Proc.*, 2769 (2023) 020056 (1-7).

[22] Z.A.A. Mahdi and K.A. Jasim, "Effect partial replacement of germanium by cadmium on dielectrically properties of $Ge_{35-x}S_{65-x}Cd_x$ chalcogenide compound", *AIP Conf. Proc.*, 3018 (2023) 020025 (1-5).

[23] K.A. Jasim et al., "The effect of neutron irradiation on the properties of $Tl_{0.6}Pb_{0.3}Cd_{0.1}Ba_2Ca_2Cu_3O_{9-\delta}$ superconductors", *Turkish J. Phys.*, 37(2) (2013) 237-241.

[24] H.M.J. Haider and K.A. Jasim, "Effect of Composition and Dielectric Properties for YBCO Superconductor Compound in Different Preparation Methods", *Ibn Al-Haitham J. Pure Appl. Sci.*, 33(1) (2020) 17-30.

[25] A.Y. Alsajjad, M.A. Mohammed and K.A. Jasim, "Preparation of Ge−Se−Sb ternary alloys

and study of the effect of antimony on electrical properties, extended and localized energy states", *AIP Conf. Proc*., 3018 (2023) 020037 (1-6).

[26] M.D. Stamate, "On the dielectric properties of DC magnetron TiO_2 thin films", *Appl. Surf. Sci.*, 218(1-4) (2003) 318-323.

[27] J.S. Mohammed et al., "Investigating the optical and electrical characteristics of $As_{60}Cu_{40-x}Se_x$ thin films", *Chalcogen. Lett.*, 20(7) (2023) 449-458.

Table (1) Values of the activation energies (E_1, E_2, and E_3) and the pre-exponential factor (σ_{oext} (σ_{01}), σ_{oloc} (σ_{02}), $\sigma o_{(f)}$ (σ_{03})) for three states of $Ge_{20}Se_{80-x}Cu_x$ chalcogenide glass system with different concentrations of Cu

Concentration	High temperature		Medium temperature		Low temperature	
x	E_1	σ_{01}	E_2	σ_{02}	E_3	σ_{03}
0	1.06	4.1×10^{-3}	0.017	2.48×10^{-6}	0.016	1.3×10^{-10}
5	1.14	2.6×10^{-3}	0.13	5.94×10^{-5}	0.012	2.92×10^{-11}
10	1.37	2.79×10^{-2}	0.012	1.62×10^{-4}	0.0125	2.83×10^{-11}
15	1.42	4.71×10^{-1}	0.09	8.87×10^{-3}	0.0157	2.96×10^{-10}

Table (2) The composition dependence values of tail width (ΔE), R, a, $N(E_{ext})$, $N(E_{loc})$, and N(EF) for a chalcogenide glass system $Ge_{20}Se_{80-x}Cu_x$ (x = 0, 5, 10, and 15) in relation to Cu concentration

x	Tail Width ΔE (eV)	R (A^0)	a (A^0)	$N(E_{ext})$ ($ev^{-1}cm^{-3}$)	$N(E_{loc})$ ($ev^{-1}cm^{-3}$)	$N(E_F)$ ($ev^{-1}cm^{-3}$)
0	1.043	13.24	26.61	1.32×10^{17}	2.72×10^{11}	1.26×10^{10}
5	1.01	11.31	41.9	8.45×10^{16}	5.27×10^{12}	2.37×10^{10}
10	1.358	11.7	3.91	9.025×10^{17}	4.05×10^{13}	2.7×10^{10}
15	1.33	10.16	0.231	1.52×10^{19}	4.575×10^{15}	3.64×10^{10}

